Diyala Journal of Engineering Sciences

ISSN 1999-8716

Vol. 02, No. 02, pp. 88-104, December 2009

Finite Element Analysis of Reinforced Concrete Beams Strengthened with CFRP In Flexural

Amer M. Ibrahim, Wissam D. Salman

College of Engineering, University of Diyala, Iraq
(Received:5/8/2009; Accepted:7/10/2009)

ABSTRACT - Numerical analyses are performed using the ANSYS finite element program to simulate reinforced concrete beams strengthened by carbon fiber reinforced polymer applied at the bottom of these beams. Nonlinear material behavior, as it relates to steel reinforcing bars and plain concrete, and linear behavior for carbon fiber reinforced polymer is simulated using appropriate constitutive models. The results showed that the general behavior of the finite element models represented by the load-deflection curves at midspan show good agreement with the test data from the previous researches. Also, the crack patterns at the failure loads from the finite element models correspond well with the observed failure modes of the experimental beams. The Finite element models represented by this research can be used to work parametric study for the strengthening of beams with CFRP.

Keywords: Finite element modeling; Reinforced concrete beams; Carbon Fiber-Reinforced Polymers.

1-INTRODUCTION:

In recent years, strengthening of reinforced concrete beams with FRP composites has been emerged as an attractive alternative to the strengthening with steel plates, because of the attractive mechanical properties of FRP composites such as, high tensile strength, high resistance for corrosion, ease of application and low cost mountainous [1,2] . Bonding FRP reinforcement to the tension face of a concrete flexural member with fibers oriented along the length of the member will provide an increase in flexural strength. Many experimental researches in this scope were presented, David, et al [3] , Minh et al [4] Harik and Choo [5] and others researchers tested beams bonded with externally CFRP strips and their results show that CFRP is very effective for flexure strengthening. On the other hand, as compared with

experimental researches, the theoretical researches are very little, Hsuan-Teh Hu [6] simulated beams strengthened with CFRP in finite element method using ABAQUS program, the resulting nonlinear constitutive equations for the FRP are coded in FORTRAN language as a subroutine and linked to the ABAQUS program.

In this paper, the ANSYS finite element program[7] is used to simulate eight full scale reinforced concrete beams tested by M. R. Esfahani et al[8].

2- M. R. ESFAHANI ET AL. EXPERIMENTAL TEST [8].

For the beam specimens, the design compressive strength of 25 MPa was used. The yield and ultimate strength of different bars are given in Table 1.

Table(1):- Test result of steel reinforcement bars

Bar diameter (mm)	8	10	12	16	20
Yielding stress (N/mm^2)	350	365	400	406	350
Ultimate stress (N/mm^2)	459	572	578	583	570

CFRP sheets were used for strengthening the beams. Mechanical properties of CFRP sheets were measured according to ASTM D3039 Standard[9]. Table 2 presents the mechanical properties of CFRP sheets.

Table(2):- Mechanical properties of CFRP sheet

Layer thickness (mm)	Ultimate strain	Tension strength (N/mm^2)	Modulus of elasticity (kN/mm^2)
0.176	0.0120	2845	237

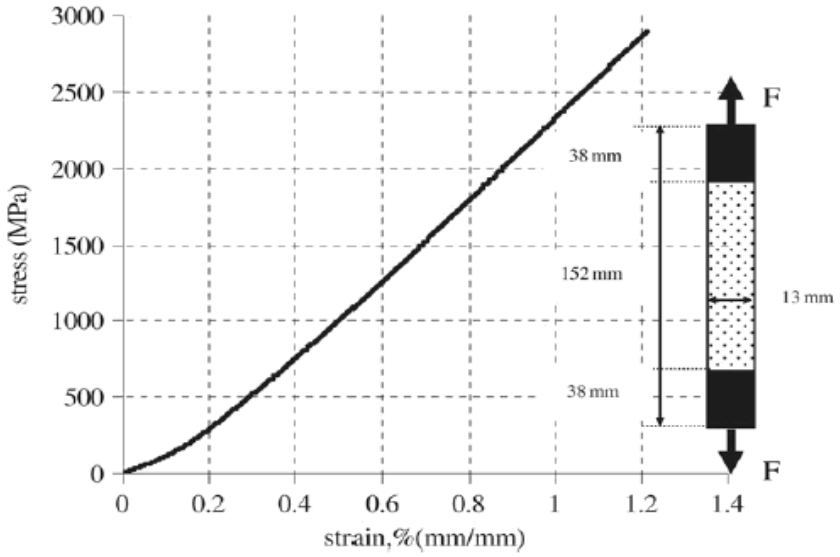

Fig.(1):- stress-strain relationship of CFRP specimen

The stress–strain relationship of CFRP sheets is shown in Fig.(1). The adhesive used for applying the CFRP sheet on the concrete surface was hand-mixed epoxy. Before applying the adhesive, the CFRP sheet was cut to length; the bottom sides of the specimens were prepared by removing any concrete surface irregularities and loose particles in order to make it a smooth surface. The adhesive was applied evenly on the concrete surface using a brush. The CFRP sheet was then smoothly hand-laid to achieve a wrinkle-free surface. The air between the concrete surface and CFRP sheet was removed using a plastic roller. Finally, a layer of adhesive was applied on the CFRP sheet for better adhesion. The adhesive curing time was at least one week, according to the manufacturer's instructions[8]. Testing of the first specimen started after one week[8].

Table(3):- Details of beam specimens

Specimens	CFRP width (mm)	CFRP layer numbers	f_c' (N/mm^2)	As (mm^2)	As' (mm^2)	d (mm)	d' (mm)
B5-16D-0L	0	0	23.8	402	157	164	25
B6-16D-1L10	100	1	23.8	402	157	164	25
B7-16D-1L15	150	1	23.8	402	157	164	25
B8-16D-2L15	150	2	23.8	402	157	164	25
B9-20D-0L	0	0	24.1	628	157	162	25
B10-20D-1L10	100	1	24.1	628	157	162	25
B11-20D-1L15	150	1	24.1	628	157	162	25
B12-20D-2L15	150	2	24.1	628	157	162	25

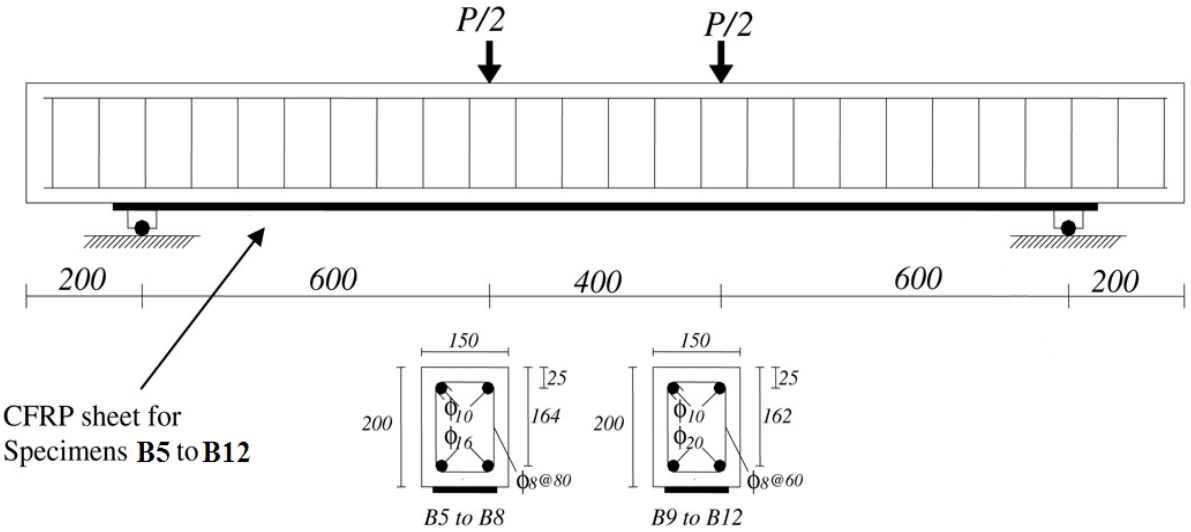

Fig.(2):- Details of beam specimens(8)

As shown in Fig.(2) and Table 3, six specimens were strengthened using CFRP sheets. The number of layers and the width of CFRP sheets varied in different specimens. Two specimens were kept without strengthening as control specimens. Specimens are named as Ba-bD-cLd. The letters a, b, c, and d refer to beam number, tensile bar diameter, the number of layers and width of CFRP sheet, respectively.

3- MATERIAL PROPERTIES AND CONSTITUTIVE MODELS

3.1- Element types

An eight-node solid element, Solid65, was used to model the concrete. The solid element has eight nodes with three degrees of freedom at each node – translations in the nodal local x, y, and z directions. The element is capable of plastic deformation, cracking in three orthogonal directions, and crushing. The geometry and node locations for this element type are shown in Figure (3).

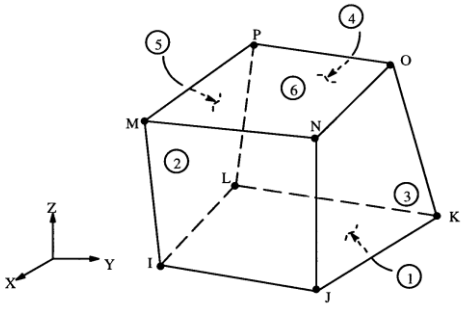

Fig.(3):- Solid65 element

A Link8 element was used to model the steel reinforcement. Two nodes are required for this element. Each node has three degrees of freedom, – translations in the nodal x, y, and

z directions. The element is also capable of plastic deformation. The geometry and node locations for this element type are shown in Figure (4)

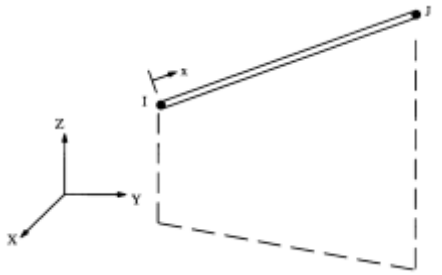

Fig.(4):- Link8 element

A layered solid element, Solid46, was used to model the FRP composites. The element allows for up to 100 different material layers with different orientations and orthotropic material properties in each layer. The element has three degrees of freedom at each node which are translations in the nodal x, y, and z directions. The geometry, node locations, and the coordinate system are shown in Figure(5).

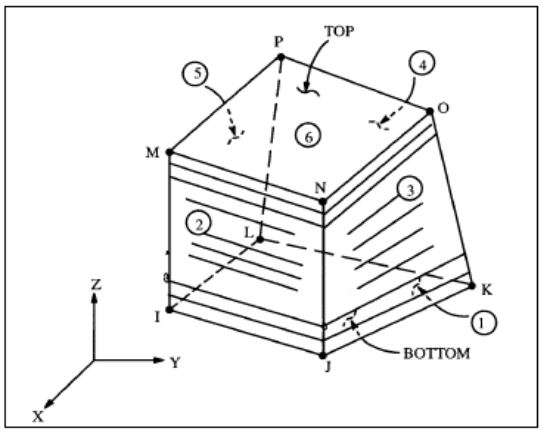

Fig.(5):- Solid46 element

An eight-node solid element, Solid45, was used for the steel plates at the supports in the beam models. The element is defined with eight nodes having three degrees of freedom at each node which are translations in the nodal x, y, and z directions The geometry and node locations for this element and the coordinate system are shown in Figure (6).

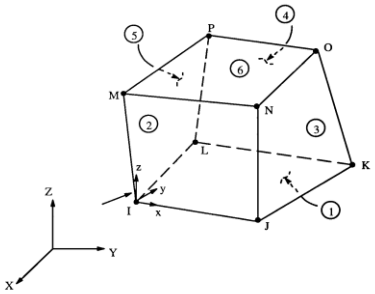

Fig.(6):- Solid 45 element

3.2- Modeling of material properties

3.2.1. Concrete

In compression, the stress-strain curve for concrete is linearly elastic up to about 30 percent of the maximum compressive strength. Above this point, the stress increases gradually up to the maximum compressive strength. After it reaches the maximum compressive strength σ_{cu} , the curve descends into a softening region, and eventually crushing failure occurs at an ultimate strain ε_{cu} . In tension, the stress-strain curve for concrete is approximately linearly elastic up to the maximum tensile strength. After this point, the concrete cracks and the strength decreases gradually to zero**.** Figure (7**)** shows Typical uniaxial compressive and tensile stress-strain curve for concrete.

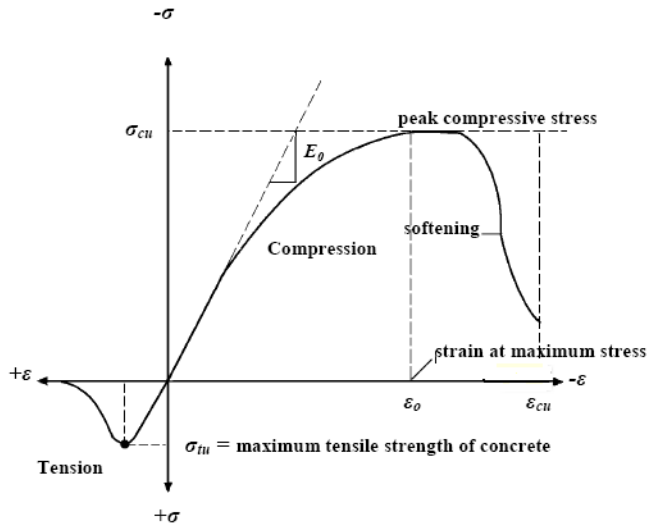

Fig.(7):- Typical uniaxial compressive and tensile stress-strain curve for concrete

The present study assumed that the concrete is a homogeneous and initially isotropic. The compressive uniaxial stress-strain relationship for concrete model is obtained by using the following equations to compute the multilinear isotropic stress-strain curve for the concrete [10,11] shown in figure 8[12].

$$f_c = \varepsilon E_c \qquad for \qquad 0 \le \varepsilon \le \varepsilon_1 \qquad (1)$$

$$f_c = \frac{\varepsilon E_c}{1+\left(\frac{\varepsilon}{\varepsilon_o}\right)^2} \qquad for \qquad \varepsilon_1 \le \varepsilon \le \varepsilon_\circ \qquad (2)$$

$$f_c = f_c^{'} \qquad for \qquad \varepsilon_\circ \le \varepsilon \le \varepsilon_{cu} \qquad (3)$$

$$\varepsilon_o = \frac{2 f_c^{'}}{E_c} \qquad (4)$$

The simplified stress-strain curve for each beam model is constructed from six points

connected by straight lines. The curve starts at zero stress and strain. Point 1, at $0.3\ f_c'$, is calculated for the stress-strain relationship of the concrete in the linear range (must satisfy Hooke's law). Points 2, 3, and 4 are obtained from Equation 2, in which ε_o is calculated from Equation 4. Point 5 is at ε_o and f_c'. The behavior is assumed to be perfectly plastic after point 5[13].

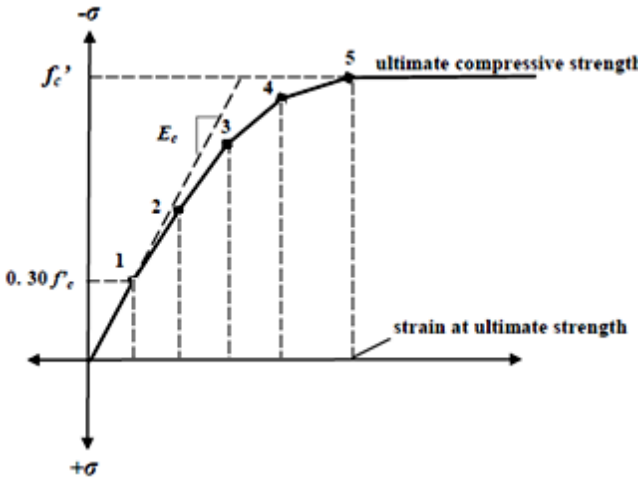

Fig.(8):- Simplified compressive uniaxial stress-strain curve for concrete

3.2.2- Steel

Steel was assumed to be an elastic-perfectly plastic material and identical in tension and compression. Poisson's ratio of 0.3 was used for the steel reinforcement in this study Figure (9) shows the stress-strain relationship used in this study. Material properties for the steel reinforcement for all eight models are as follows:

Elastic modulus, E_s = 200,000 MPa, Poisson's ratio (0.3).

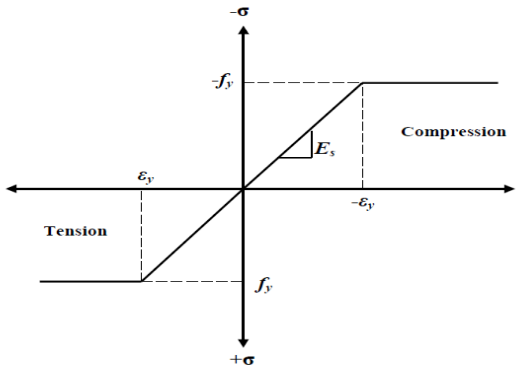

Fig.(9):- Stress-strain curve for steel reinforcement

3.2.3- Carbon Fiber Reinforced polymer

FRP composites are materials that consist of two constituents. The constituents are combined at a macroscopic level and are not soluble in each other. One constituent is the reinforcement, which is embedded in the second constituent, a continuous polymer called the

matrix. The reinforcing material is in the form of fibers, i.e., carbon and glass, which are typically stiffer and stronger than the matrix. The FRP composites are anisotropic materials; that is, their properties are not the same in all directions. Figure (10) shows a schematic of FRP composites.

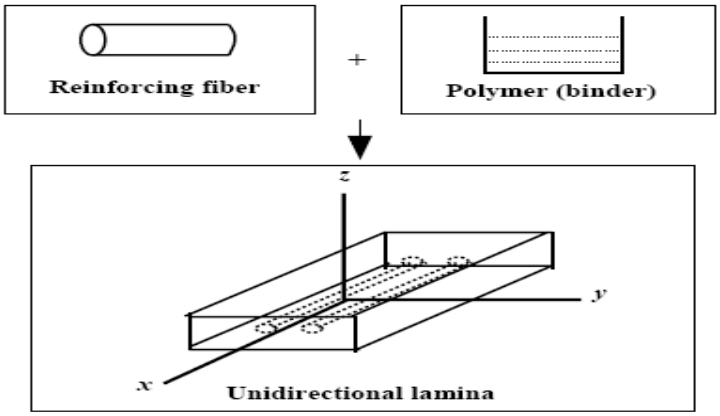

Fig.(10):- shows a schematic of FRP composites

Linear elastic properties of the CFRP composites were assumed throughout this study. Figure (11) shows the stress-strain curves used in this study for the FRP composites in the direction of the fiber.

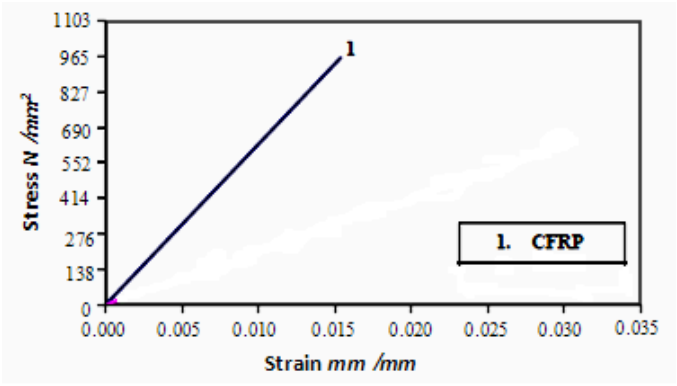

Fig.(11):- Stress-strain curves for the FRP composites in the direction of the fibers

4- NUMERICAL ANALYSIS AND COMPARISON OF RESULTS

4.1 Load-Deflection curves

Deflections are measured at midspan at the center of the bottom face of the beams. Figures (12) to (19) show the load-deflection curves for the control and flexural-strengthened beams for experimental [8] and analytical results. In general, the load deflection curves for the beams from the finite element analyses agree quite well with the experimental data. The finite element load deflection curves in the linear range are somewhat stiffer than the experimental plots. After first cracking, the stiffness of the finite element models is again higher than that

of the experimental beams. There are several effects that may cause the higher stiffnesses in the finite element models. First, microcracks are present in the concrete for the experimental beams, and could be produced by drying shrinkage in the concrete and/or handling of the beams. On the other hand, the finite element models do not include the microcracks. The microcracks reduce the stiffness of the experimental beams. Next, perfect bond between the concrete and steel reinforcing is assumed in the finite element analyses, but the assumption would not be true for the experimental beams. As bond slip occurs, the composite action between the concrete and steel reinforcing is lost. Thus, the overall stiffness of the experimental beams is expected to be lower than for the finite element models (which also generally impose additional constraints on behavior).

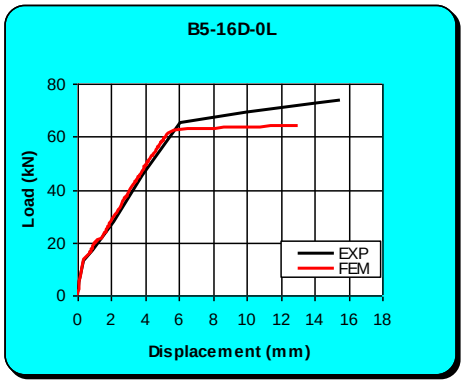

Fig.(12):- Load-deflection curve of beam (B5)

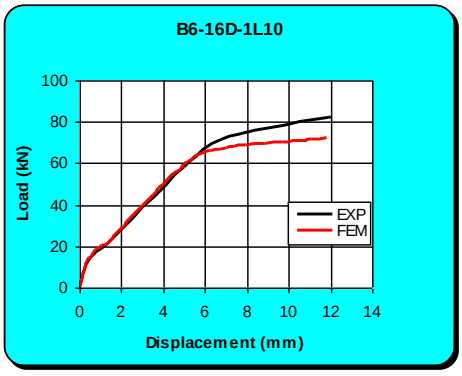

Fig.(13):- Load-deflection curve of beam (B6)

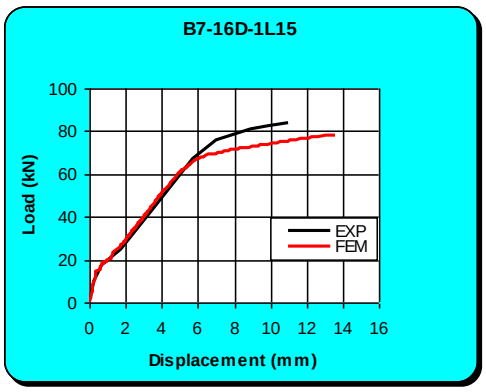

Fig.(14):- Load-deflection curve of beam (B7)

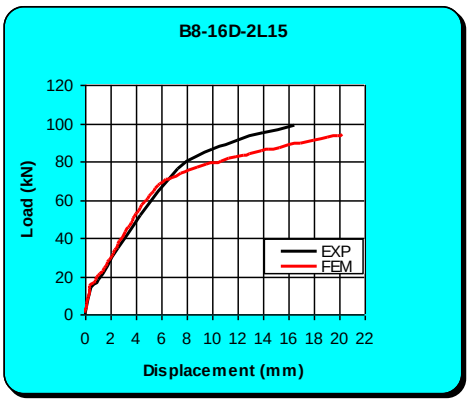

Fig.(15):- Load-deflection curve of beam (B8)

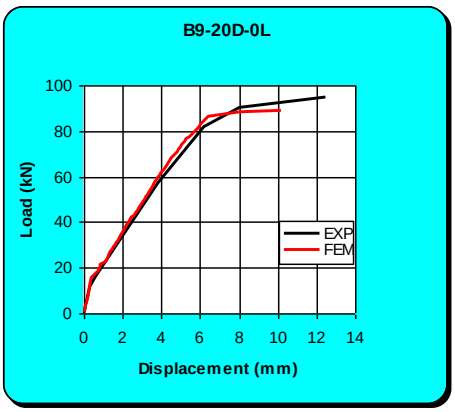

Fig.(16):- Load-deflection curve of beam (B9)

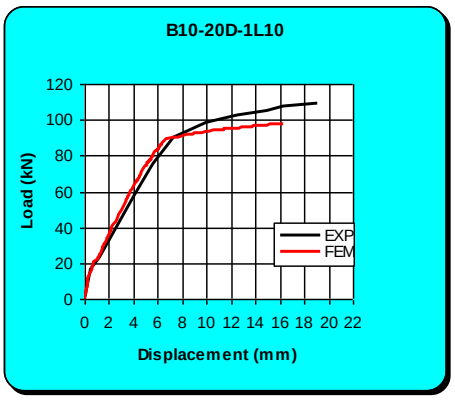

Fig.(17):- Load-deflection curve of beam (B10)

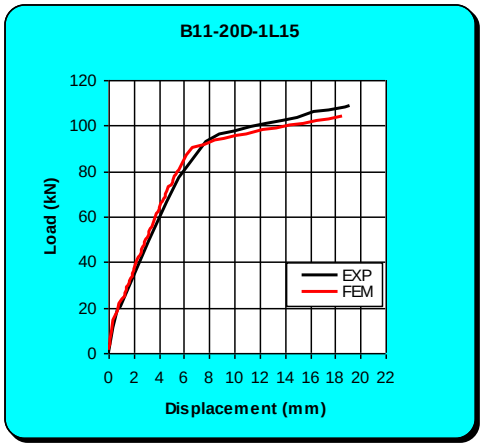

Fig.(18):- Load-deflection curve of beam (B11)

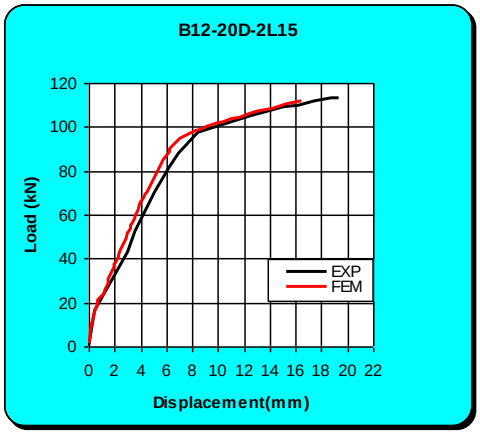

Fig.(19):- Load-deflection curve of beam (B12)

4.2- Stresses and Strain Distribution in Beams

Figure (20) shows the predicted stress distribution in concrete for beam (B11) along a section of mid-span of the beam at various stages of loading. The stress distribution in concrete at the early stages was linear. After cracking load the distribution of concrete stress becomes nonlinear. As the load is increased, position of the neutral axis is shifted toward the compression zone of the cross section. The increase in concrete strain of beam along a section of the beam at various stages of loading is also presented in Figure (21). the variation of strain was almost linear until failure. The linear variation of strain can be attributed to the proper anchorage of the CFRP sheet to the supports. The proper anchorage prevented the debonding of CFRP sheet from concrete.

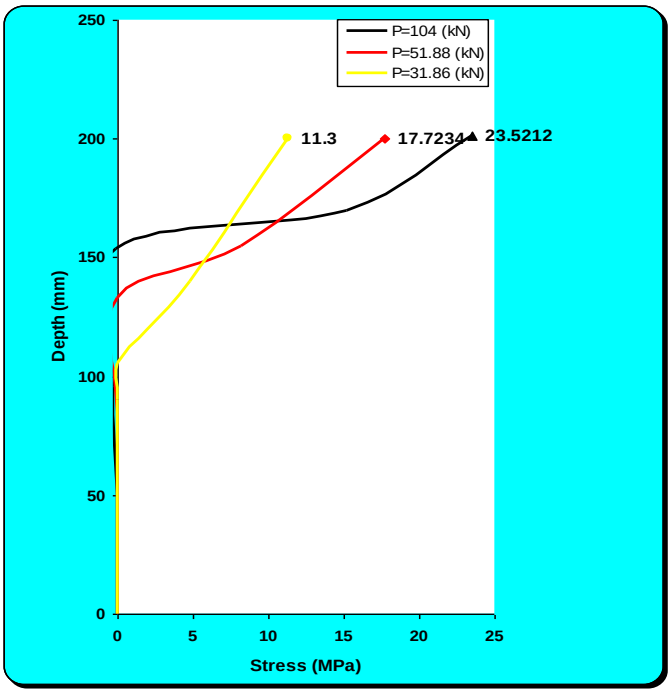

Fig.(20):- Stress Distribution for Concrete Section of beam (11)

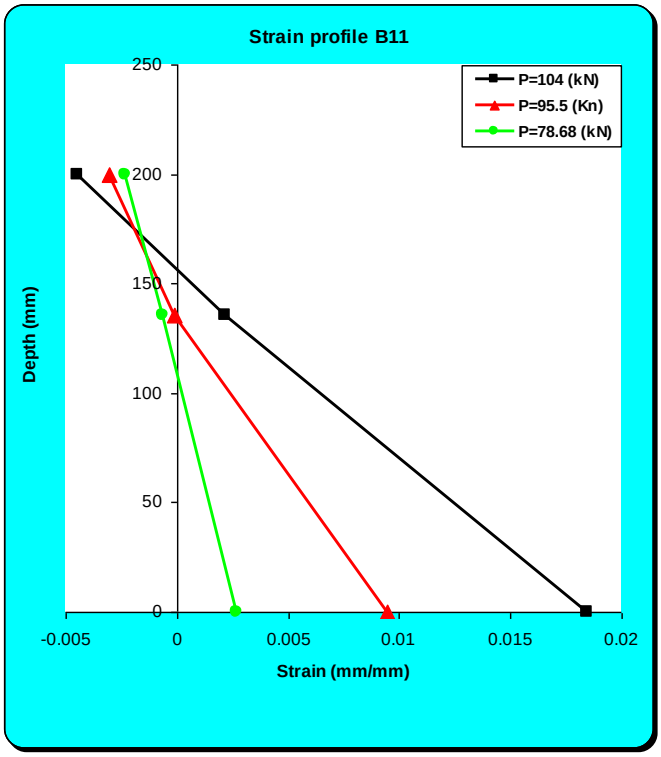

Fig.(21):- Strain Distribution for beam (11)

4.3 Crack pattern

The ANSYS program records a crack pattern at each applied load step. Figures (22) to (24) shows evolutions of crack patterns developing for each beam at the last loading step. ANSYS program displays circles at locations of cracking or crushing in concrete elements.

Cracking is shown with a circle outline in the plane of the crack, and crushing is shown with an octahedron outline. The first crack at an integration point is shown with a red circle outline, the second crack with a green outline, and the third crack with a blue outline [7]. And these figures show comparison of cracks patterns between experimental beams and finite element beams at failure load. In general, flexural cracks occur early at midspan. When applied loads increase, vertical flexural cracks spread horizontally from the midspan to the support. At a higher applied load, diagonal tensile cracks appear. Increasing applied loads induces additional diagonal and flexural cracks. Finally, compressive cracks appear at nearly the last applied load steps.

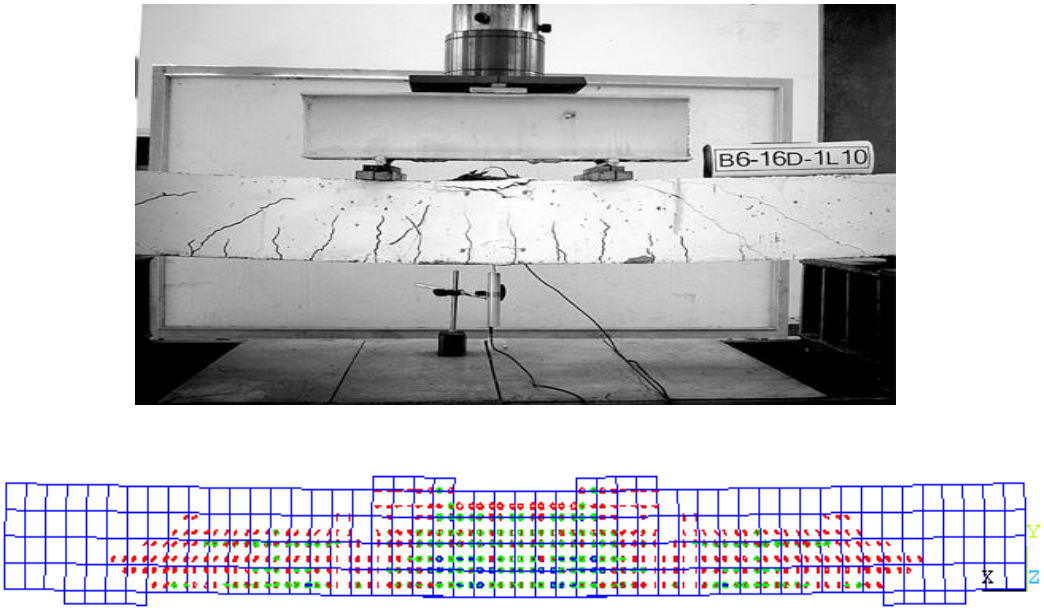

Fig.(22):- Cracks patterns in beam (6) and finite element model of beam(6)

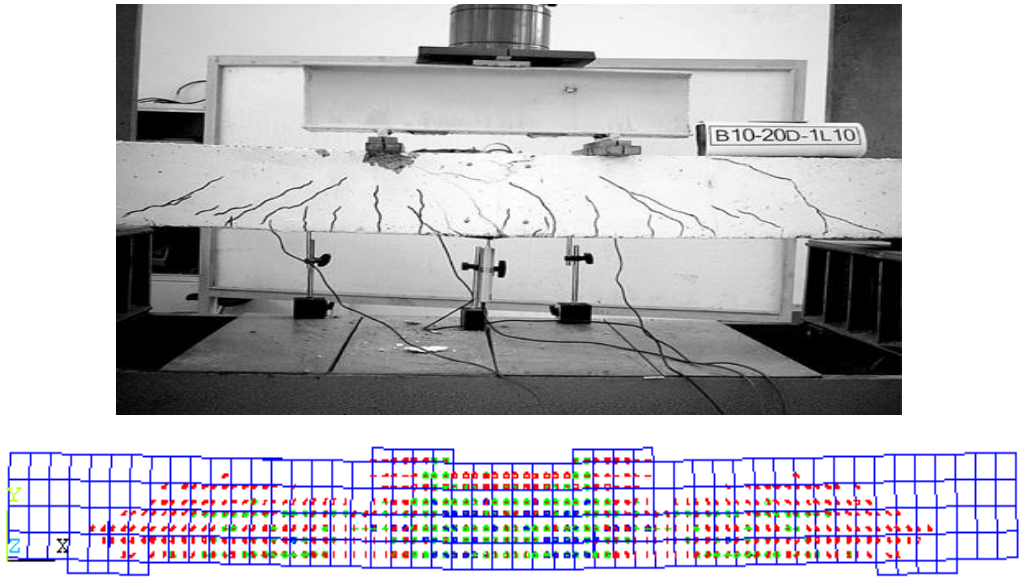

Fig.(23):- Cracks patterns in beam (10) and finite element model of beam(10)

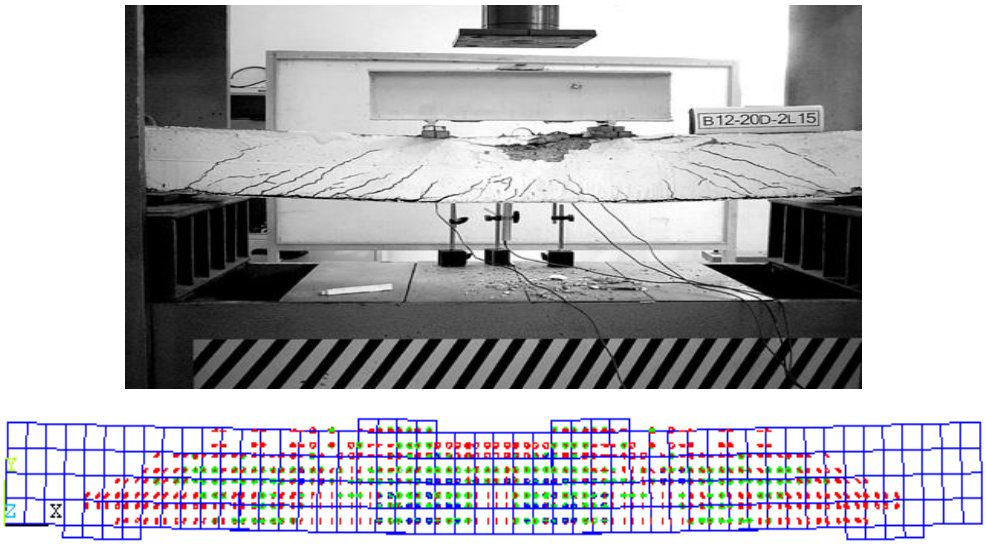

Fig.(24):- Cracks patterns in beam (12) and finite element model of beam(12)

The failure modes of the finite element models show good agreement with observations and data from the experimental full-scale beams. The addition of FRP reinforcement to the control beam shifts the behavior of the beams from a shear failure near the ends of the beam to flexure failure at the midspan.

4.4 Loads at Failure

Table 5 shows comparisons between the ultimate loads of the experimental beams [8] and the final loads from the finite element models. The final loads for the finite element models at the last applied load steps before the solution diverges due to numerous cracks and large deflections. It is seen that the ANSYS models underestimate the strengths of the beams, as anticipated. One explanation is that the toughening mechanisms at the crack faces, i.e. the grain bridging process, interlocking between the cracked faces, crack tips blunted by voids, and the crack branching process, may also slightly extend the failures of the experimental beams before complete collapse. The finite element models do not have these mechanisms. Finally, the material properties and (model) assumed in this study may be imperfect.

Table (5): Comparisons between the ultimate loads of the experimental beams [8] and the final loads from the finite element models.

Beam	Experimental[8] ultimate load (kN)	Numerical ultimate load (kN)	% Difference	Increased in ultimate load of strengthened
B5-16D-0L	75.94	64	15.7	1.00
B6-16D-1L10	84.93	72	15.2	1.13
B7-16D-1L15	94.92	78.4	17.4	1.23
B8-16D-2L15	105.91	94	11.2	1.47
B9-20D-0L	96.42	88.8	7.9	1.00
B10-20D-1L10	106.32	98	7.8	1.10
B11-20D-1L15	108.91	104	4.5	1.17
B12-20D-2L15	113.41	112	1.2	1.26

5- CONCLUSIONS

In this paper, nonlinear finite element analyses of rectangular reinforced concrete beams strengthened by CFRP are performed. Based on the numerical results, the following conclusions may be drawn:

1. The general behavior of the finite element models represented by the load-deflection curves at midspan show good agreement with the test data from the full-scale beam tests. However, the finite element models show slightly more stiffness than the test data in both the linear and nonlinear ranges. The effects of bond slip (between the concrete and steel reinforcing) and microcracks occurring in the actual beams were excluded in the finite element models, contributing to the higher stiffness of the finite element models.
2. The final loads from the finite element analyses are lower than the ultimate loads from the experimental results. This is probably due ignoring the effects of concrete toughening mechanisms; and using assumed materials properties values instead of measured values.
3. The load carrying capacity of the Flexure strengthened beam predicted by the finite element analysis is higher than that of the Control Beam.

4. The crack patterns at the final loads from the finite element models correspond well with the observed failure modes of the experimental beams.

REFERENCES

1. ACI Committee 440F. Guide for the design and construction of externally bonded FRP systems for strengthening concrete structures. 2002.
2. ACI 318M-05, American Concrete Institute,(2005) Building Code Requirements for Reinforced Concrete, American Concrete Institute, Farmington Hills, Michigan.
3. David ,E.,Djelal, C. and Buyle-Bodin , F., " Repair and Strengthening of Reinforced Concrete Beams using Composite Matreials",second Int. PhD. Symposium in Civil Engineering, 1998 Budapest, WWW.vbt.bme.hu.
4. Minh,N.D.,Khan,C.T. and Kiat, C.H," Effect of Plate Length on The Strength of Reinforced Concrete Beams Bounded with CFRP plates ",School of Civil and Structural Engineering , Nanyang Technological University 1998.
5. P. Alagusundaramoorthy, I. E. Harik, and C.C. Choo,(2002) Shear strength of R/C beams wrapped with CFRP fabric Kentucky transportation center, college of engineering, 2002.
6. Hsuan-Ten Hu , Fu-ming lin, Yih-yuan Jan ,(2004),"Nonlinear Finite Element Analysis of Reinforced Concrete Beams Strengthened by Fiber Reinforced Composite Structure 63,pp 271-281.
7. Ansys Manual , Version 10.0
8. M. R. Esfahani , M. R. Kianoush ,A. R. Tajari , (2006) ," Flexural Behavior of Reinforced Concrete Beams Strengthened by CFRP Sheets" , Engineering Structure.
9. ASTM D3039 ,Standard Test Method for Tensile Properties of Polymer Matrix Composite Materials", West Conshohocken ,(Pennsywania) : American Society for Testing and Materials,1995.
10. Desayi, P. and Krishnan, S., (1964) Equation for the Stress-Strain Curve of Concrete, Journal of the American Concrete Institute, 61, pp. 345-350, March.
11. Gere, J. M. and Timoshenko, S. P.,(1997) Mechanics of Materials, PWS Publishing Company, Boston, Massachusetts.
12. Wolanski A. J.,(2004) Flexural Behavior of Reinforced and Prestressed Concrete Beams using Finite Element Analysis, M.Sc. Thesis, University of Marquette, May .

13. Kachlakev , D. I. and Mccurry D.I. ,"Simulated Full Scale Testing of Renforced Concrete Beams Strengthened with FRP Composite: Experimental Results and Design Model Verification " United State Department of Transportation , Fedral Highway Administration.

Notations

f_c'	Ultimate uniaxial compressive strength	(N/mm^2)
E_c	Concrete elastic modulus	(N/mm^2)
E_s	Steel elastic modulus	(N/mm^2)
f_c	stress at any strain ε	(N/mm^2)
f_r	Concrete modulus of rupture	(N/mm^2)
ε	Strain	
ε_1	strain corresponding to ($0.3f_c'$)	
ε_{cu}	ultimate compressive strain	
ε_o	Strain at the ultimate compressive strength f_c'	

استخدام طريقة العناصر المحددة لتحليل العتبات الخرسانية المسلحة المقواة بألياف الكربون المسلح بالبوليمر في حالة الانثناء

د. عامر محمد إبراهيم
أستاذ مساعد
كلية الهندسة ـ جامعة ديالى

وسام داود سلمان
مدرس مساعد
كلية الهندسة ـ جامعة ديالى

الخلاصة

لقد استخدم التحليل العددي (طريقة العناصر المحددة باستخدام برنامج ANSYS) لمحاكاة أو لتمثيل العتبات الخرسانية المسلحة المقواة بألياف الكربون المسلح بالبوليمرالمثبتة في أسفل العتبات.سلوك المواد كان غير خطيا بالنسبة لقضبان حديد التسليح والخرسانة,أما ألياف الكربون المسلح بالبوليمر فكان سلوكها خطيا للوصول إلى نماذج ملائمة وقريبة للواقع, نتائج السلوك العام للنماذج المتكونة بطريقة العناصر المحددة والتي يمثلها منحني الحمل –الانحراف في وسط العتبة أظهرت تقارب كبير مع البيانات العملية للبحوث السابقة.كما أن نمط التشقق عند الحمل النهائي لنماذج العناصر المحددة تتطابق تماما مع العتبات المفحوصة عمليا.النماذج المتكونة بطريقة العناصر المحددة في هذا البحث يمكن أن تستخدم لدراسة المحددات العملية لتقوية العتبات بألياف الكربون المسلح بالبوليمر.